



ELSEVIER

July 2002

Materials Letters 55 (2002) 67–72

**MATERIALS  
LETTERS**

www.elsevier.com/locate/matlet

# Physical and structural properties of ZnO sputtered films

Walter Water, Sheng-Yuan Chu\*

*Department of Electrical Engineering, National Cheng Kung University, 1 University Rd., Tainan, Taiwan*

Received 7 May 2001; received in revised form 5 July 2001; accepted 1 October 2001

## Abstract

In this paper, poly-crystal zinc oxide (ZnO) films with *c*-axis (002) orientation have been successfully grown on the silicon substrate by r.f. magnetron sputtering technique. The deposited films were characterized as a function of deposition temperature, argon–oxygen gas flow ratio, and r.f. power. Crystalline structures, stress and roughness characteristics of the films were investigated by X-ray diffraction (XRD), scanning electron microscopy (SEM) and atomic force microscopy (AFM) measurement. By controlling deposition parameters and annealing temperature, we could improve intrinsic stress and surface roughness of ZnO film. Preferred deposition condition was found to show good film quality for SAW device applications. © 2002 Elsevier Science B.V. All rights reserved.

**Keywords:** ZnO; r.f. sputtering; Annealing; SAW; XRD; SEM; AFM

## 1. Introduction

Zinc oxide (ZnO), a semiconducting, photoconducting, piezoelectric, and optical waveguide material, shows a wide range of scientific and technological applications. It belongs to a group of the hexagonal wurtzite, 6-mm symmetry; it is an n-type wide-bandgap semiconductor material and has variety of potential applications. ZnO films also have widely been used as surface acoustic wave devices and bulk acoustic resonators due to its strong piezoelectric effect [1–5]. ZnO films can be deposited by variety deposition techniques, such as sol–gel process [6], spray pyrolysis [7], molecular beam deposition (MBE) [8], chemical vapor deposition (CVD) [9] and sputtering [10–14]. The most common-used technique is sputter-

ing because it is possible to obtain good orientation and uniform films close to single-crystal morphology even on amorphous substrate or at low substrate temperature. For SAW device applications, it is necessary for ZnO films to have high resistivity and *c*-axis oriented crystalline structure which depends on the deposition condition, such as substrate temperature, deposition power, deposition pressure and argon–oxygen flow. Silicon wafer is commonly chosen due to the potential for the development of the acoustic elements integrated with electronic circuitry.

In this paper, we try to deposit ZnO films with *c*-axis (002) orientation on the Si substrate by r.f. magnetron sputtering technique. The deposited films were characterized as a function of deposition temperature, pressure, argon–oxygen gas flow ratio, and r.f. power. Crystalline structures of the films were investigated by X-ray diffraction (XRD), scanning electron microscopy (SEM) and atomic force microscopy (AFM) measurement. Preferred deposition condition

\* Corresponding author.

E-mail address: chusy@mail.ncku.edu.tw (S.-Y. Chu).

was found to show good film quality for SAW device applications.

Investigating our data, we found some thought-provoking and significant results, which are different from those obtain from other research group. Such as the surface roughness was relative to substrate temperature. Therefore, we focus our experiments on the sputtering conditions (substrate temperature/oxygen ratio) influence on surface roughness. Since the ZnO films were grown in low pressure ( $10^{-3}$  Torr), the stress was much bigger than other groups. By post-deposition annealing process, the stress will still be free.

## 2. Experimental procedure

ZnO films were deposited by r.f. magnetron sputtering system using a Zn target (99.99%) with diameter of 3 in. and thickness of 6 mm. Substrate is p-type silicon with (100) orientation. The substrates were thoroughly cleaned with organic solvents and dried before loading in the sputtering system. The chamber was down to  $6 \times 10^{-6}$  Torr using diffusion pump before introducing the premixed Ar and O<sub>2</sub> sputtering gases into the chamber through a precision leak valve and controlled by the main valve of diffusion pump. Throughout all experiments, the target was presputtered for 15 min under 150-W RF power before the

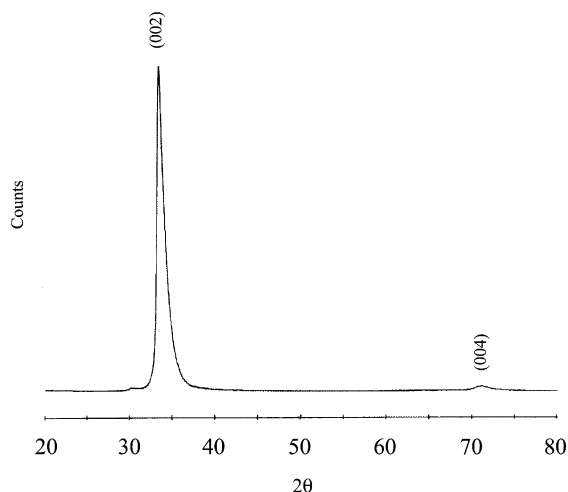
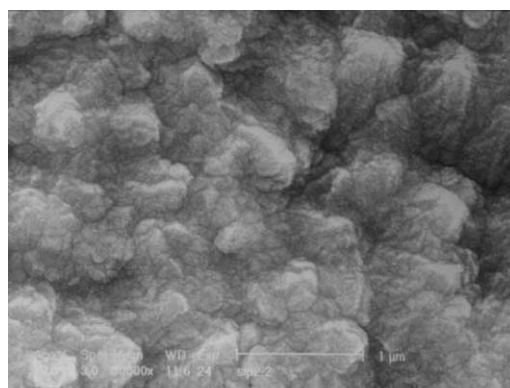


Fig. 1. X-ray pattern of ZnO film with *c*-axis (002) orientation deposited on silicon substrate.

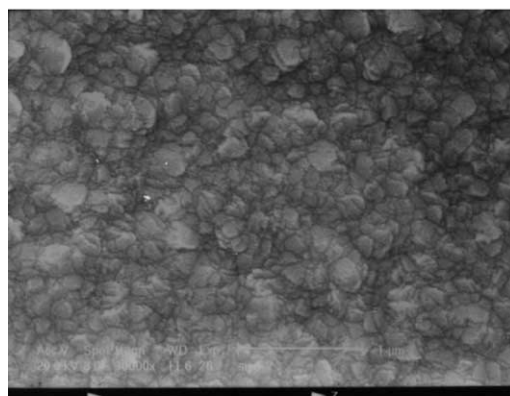
Table 1

Power	150 W
Substrate temperature	200 °C
Pressure	$3 \times 10^{-3}$ Torr
O <sub>2</sub> %	40%
Deposition time	120 min
Target-substrate distance	50 mm

actual deposition begins to delete any contamination on the target surface to make the system stable and reach optimum condition. The ratio of argon to oxygen was controlled by the electronic mass flow controller. The substrate temperature was monitored utilizing a thermo-coupler attached near the substrate. The substrate heating was initiated to attain the desired deposition temperature.



(a) ——— μm



(b) ——— μm

Fig. 2. The surface SEM picture of ZnO Films. (a) Substrate temperature is 100 °C. (b) Substrate temperature is 300 °C.

### 3. Results and discussion

#### 3.1. X-ray diffraction

Fig. 1 showed the diffraction pattern of ZnO film with strong *c*-axis (002) orientation. X-ray examination of piezoelectric films has been a major tool for determining the uniformity of crystalline structure [15]. The higher the degree of orientation of a piezoelectric, the higher the electromechanical coupling coefficient of the piezoelectric [16]. The sputtering parameters were shown in Table 1.

#### 3.2. Scanning electron microscopy

SEM observation by the secondary-electron mode revealed the layer morphology and thickness. Fig. 2 showed the surface microstructures of ZnO films grown in 100 and 300 °C substrate temperature, separately. The other sputtering conditions were the same as shown in Table 1. The film deposited in 100 °C substrate was cloudy with a rough surface. The temperature of substrate controlled the mobility of the

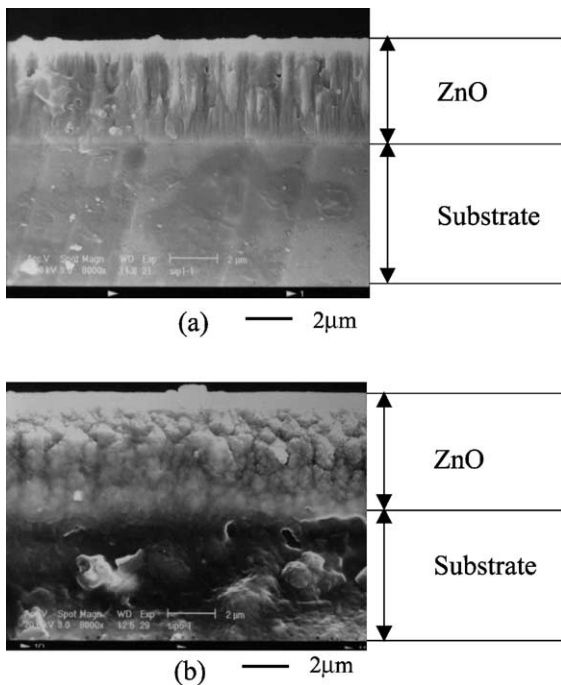


Fig. 3. Cross-sectional view of the ZnO film. (a) Substrate temperature is 100 °C. (b) Substrate temperature is 300 °C.

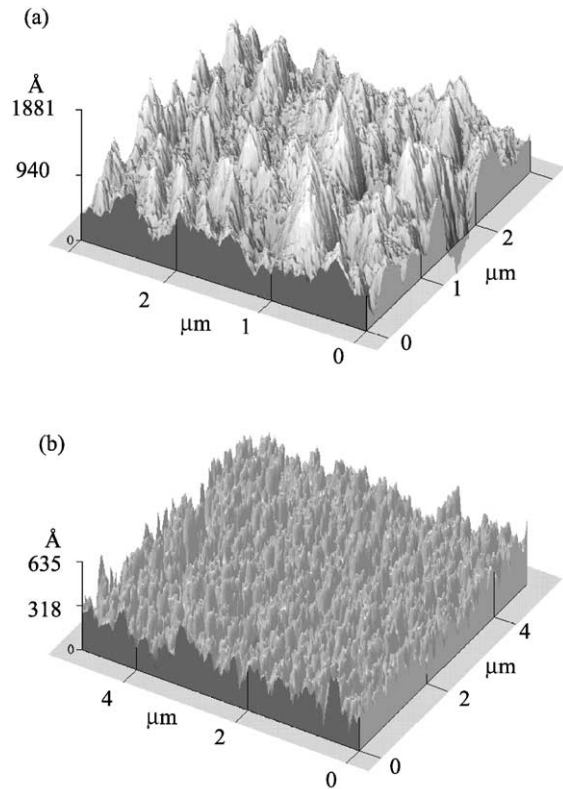


Fig. 4. AFM of ZnO films were deposited by (a) 100 °C and (b) 300 °C substrate temperature.

absorbed atoms and resulting structure of deposition film. Depositing in cool substrate with low mobility tended to form crystallite structure, which was highly porous and rough surface. On the other hand, high substrate temperature provided energy of surface atoms to enhance mobility that could improve roughness and quality of film. Therefore, the film deposited in 300 °C substrate will show finer uniform grains and smoother surface [13]. Fig. 3a showed the cross-sectional view of the Fig. 2a ZnO film. The structure, which looks columnar, was proved to have a parallel *c*-axis orientation. Fig. 3b showed the cross-sectional view of the Fig. 2b ZnO film. The structure of Fig. 3b had weaker *c*-axis (002) orientation than Fig. 3a and had other oriented crystalline. Fig. 4 demonstrates the AFM data of ZnO films in Fig. 2, the thickness of films were about 4.5–5 μm. The roughness was 93.5 Å of 300 °C substrate temperature and 263 Å of 100 °C substrate temperature.

### 3.3. Roughness of surface

As ZnO films were used for SAW device applications, the rough surface will impede wave transmission and increase propagation loss. Fig. 5 showed various roughness of the film's surface as a function of substrate temperature. The other sputtering conditions were the same as Table 1. The substrate temperature controlled the mobility of the absorbed atoms and resulting structure of deposition film. High substrate temperature provided energy of surface atoms to enhance mobility that could improve roughness and quality of film. Therefore, the film was deposited in 300 °C substrate with the finest uniform grains and smooth surface. However, the substrate temperature was too high that will cause the grain to overgrow and induce the rough surface [13].

Fig. 6 showed various roughness of the film's surface as a function of oxygen ratio. The other sputtering conditions were the same as Table 1. Investigating our data, the suitable ratio of oxygen to obtain smooth surface is 0.4 [13,17]. This maybe due to excess zinc or oxygen, which could influence the surface structure of ZnO film.

The data of Yamazaki et al.'s [18] report have shown that the smooth surface could be obtained at the lowered substrate temperature. As shown in our data, the optimum substrate temperature to obtain the smoothest surface is 300 °C, however, we found that this was not the strongest *c*-axis (002) orientation. Growing ZnO films at low substrate temperature had stronger *c*-axis (002) orientation than at high substrate

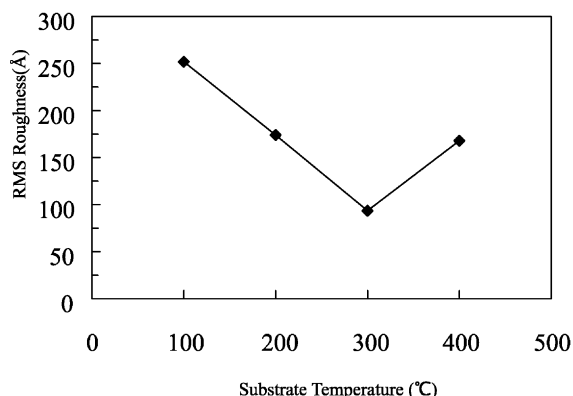


Fig. 5. Roughness of films as a function of substrate temperature.

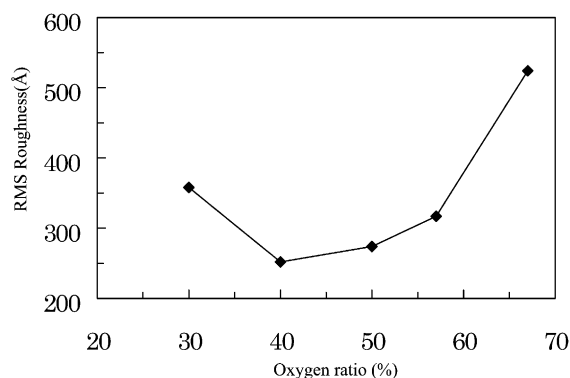


Fig. 6. Roughness of films as a function of oxygen ratio.

temperature in our experiments. Considering the film's roughness and (002) orientation, the suitable substrate temperature to deposit ZnO films is 200 °C. As to oxygen ratio, 40% oxygen can obtain the smoothest surface and the strongest *c*-axis (002) orientation in our experiments.

### 3.4. Intrinsic stress

Virtually all vacuum-deposited films are in a state of stress. The stress composed of a thermal stress and an intrinsic stress. The thermal stress is due to the difference in the thermal expansion coefficients ( $\alpha$ ) of the coating and substrate. The  $\alpha$  value of silicon being  $2.5 \times 10^{-6}/^{\circ}\text{C}$  at room temperature is noteworthy. ZnO crystal is hexagonal and its  $\alpha_{11}$  and  $\alpha_{33}$  values are 6.05 and  $3.53 \times 10^{-6}/^{\circ}\text{C}$ , respectively, as reported in Ref. [19]. Since the  $\alpha$  value of ZnO is bigger than silicon, the silicon substrate gives a tensile stress to a ZnO film as the substrate cools down from high temperature to room temperature. The intrinsic stress is due to the accumulating effect of the crystallographic flaws, which are built into the coating during growth. The compressive stresses are believed to be due to energetic argon and oxygen atoms reflected from target. The reflected atoms can be sufficiently energetic to penetrate into and become buried in the growing coating. Another reason is that argon and oxygen atoms produce the stresses by being trapped in the coating [20].

The angular peak position of ZnO powder is  $2\theta = 34.4^{\circ}$ . However, in ZnO film, the deviation of the position of the diffraction peak from its bulk-

Table 2

Substrate temperature (°C)	2θ	Lattice constant “c-axis” (Å)	Stress (10 <sup>10</sup> dyn/cm <sup>2</sup> )	Elastic constant × C <sub>33</sub> (single)
100	33.35	5.3689	13.88	0.8756
200	33.65	5.3224	9.90	0.9066
300	34.05	5.2617	4.71	0.9492
400	34.15	5.2467	3.43	0.9601

C<sub>33</sub> (single) is elastic constant C<sub>33</sub> of single crystal ZnO.

type's value is mainly due to the compressive strain produced within the film. The angular peak position of the deposited film is less than that of the bulk-type's value. This is because of the uniform state of stress with compressive components parallel to substrate. The stress in sputtered ZnO films investigated by various workers has been found associated with interstitial oxygen [14,17,19–21]. The compressive stress would change the elastic constant C<sub>33</sub> value. The elastic constant C<sub>33</sub> plays an important role in SAW devices; it will change the acoustic wave velocity and the corresponding electromechanical coupling constant  $k^2$ . The estimated values of lattice constant, stress and C<sub>33</sub> were listed in Table 2.

The lattice constant can be used to evaluate the average uniform strain,  $e_{ZZ}$  in the lattice along the *c*-axis [14]

$$e_{ZZ} = (C_0 - C)/C_0 \quad (1)$$

where *C* is the lattice constant obtained from the (002) reflection in the X-ray and *C*<sub>0</sub>, the corresponding bulk value. The stress in the plane of the film is [14]

$$\sigma = [2C_{13} - (C_{11} + C_{12})C_{33}/C_{13}]e_{ZZ} \quad (2)$$

the elastic constant of the film is [14,22]

$$(C_{33})_{\text{film}} = 0.99C_{33}/(1 - e_{ZZ})^4 \quad (3)$$

Fig. 7 displayed the various stresses as a function of substrate temperature. The sputtering conditions of original ZnO films were the same as shown in Table 1. In low substrate temperature (100 °C), a very strong planar compressive stress exists in ZnO film. The negative sign means that the stress is in compression condition. Increasing substrate temperature, the compressive stress would be relieved because the defects of the film will be decreased and the oxygen will be

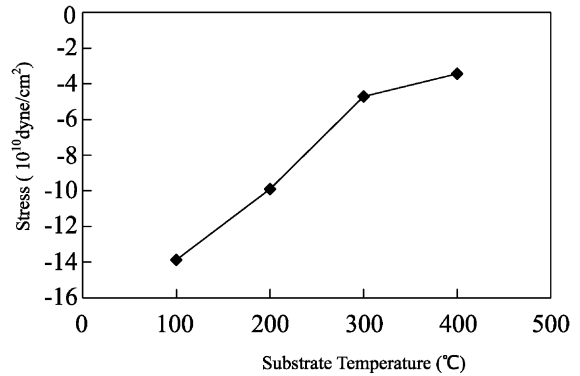


Fig. 7. Stress of films as a function of substrate temperature.

out-diffused caused by thermal expansion. Another reason is that the thermal expansion coefficient of ZnO is bigger than that of Si, a tensile stress was given for Si substrate.

Relieving the stress, postdeposition annealing is a popular method. During annealing process, the atoms of ZnO have energy to rearrange and will reduce the intrinsic stress. On the other hand, the thermal expansion coefficient of ZnO is bigger than that of Si, the tensile stress of silicon and compressive stress of intrinsic stress will cancel out each other. Since the ZnO films were grown during low sputtering pressure ( $3 \times 10^{-3}$  Torr), the stress of films was bigger than the other groups [14,19,23]. In Fig. 8, we find that the annealing temperature about 600 °C 1 h in air will make the stress free.

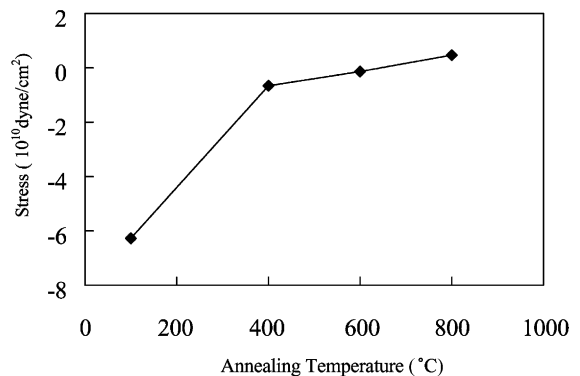


Fig. 8. Stress of films as a function of annealing temperature.

#### 4. Conclusion

For piezoelectric device applications, ZnO films should have *c*-axis oriented crystalline structure and smooth surface. However, the optimum sputtering condition to obtain the smoothest surface cannot get the strongest *c*-axis orientation. The suitable substrate temperature to grow ZnO films is 200 °C and the optimum oxygen ratio is 40%. The stress of ZnO film has been relieved by annealing process. The use of ZnO layer with Si substrate will enable one to monolithically integrate surface acoustic wave (SAW) devices with semiconductor electronics. Crystalline structures and orientations of the films were investigated. By controlling sputtering substrate temperature and argon–oxygen gas flow ratio could obtain the suitable ZnO films for SAW device applications.

#### Acknowledgements

This research was supported by the National Science Council of Republic of China, under grant NSC89-2213-E006-209.

#### References

- [1] S.J. Martin, et al., *Ultrason. Symp.* (1980) 113.
- [2] O. Yamazaki, T. Mitsuyu, K. Wasa, *IEEE Trans. Sonics Ultrason.* SU-27 (6) (November 1980) 369.
- [3] J.H. Visser, M.J. Vellekoop, A. Venema, E. van der Drift, P.J.M. Rek, A.J. Nederlof, M.S. Nieuwenhuizen, *Ultrason. Symp.* (1989) 195.
- [4] J. Koike, K. Shimoe, H. Ieki, *Jpn. J. Appl. Phys.* 32 (Pt. 1, No. 5B) (1993) 2337.
- [5] M. Kadota, C. Kondoh, *IEEE Trans. Ultrason. Ferroelectr. Freq. Control* 44 (3) (May 1997) 958.
- [6] M.N. Kamalasanan, S. Chandra, *Thin Solid Films* 288 (1996) 112.
- [7] F.D. Paraguay, W.L. Estrada, D.R.N. Acosta, E. Andrade, M. Miki-Yoshida, *Thin Solid Films* 350 (1) (1999) 192.
- [8] K. Nakamura, T. Shoji, K. Hee-Bog, *Jpn. J. Appl. Phys., Part 2: Letters* 39 (6) (2000) L534.
- [9] T. Minami, H. Sonohara, S. Takata, H. Sato, *Jpn. J. Appl. Phys., Part 2: Letters* 33 (5B) (May 15, 1994) L743.
- [10] S. Maniv, A. Zangvil, *J. Appl. Phys.* 49 (5) (May 1978) 2787.
- [11] M.-S. Wu, W.-C. Shih, W.-H. Tsai, *J. Phys. D: Appl. Phys.* 31 (1998) 943.
- [12] K. Hashimoto, S. Ogawa, A. Nonoguchi, T. Omori, M. Yamaguchi, *IEEE Ultrason. Symp.* (1998) 207.
- [13] K.B. Sundaram, A. Khan, *Thin Solid Films* 295 (1997) 87.
- [14] V. Gupta, A. Mansingh, *J. Appl. Phys.* 80 (2) (15 July 1996) 1063.
- [15] S. Fred, S. Hickernell, *IEEE Ultrason. Symp. Proc.* (1996) 235.
- [16] M. Akiyama, H.R. Kokabi, K. Nonaka, K. Shobu, T. Watanabe, *J. Am. Ceram. Soc.* 78 (1995) 3004.
- [17] K. Sugiyama, et al., *J. Mater. Sci. Lett.* 9 (1990) 489.
- [18] O. Yamazaki, T. Mitsuyu, K. Wasa, *IEEE Trans. Sonics Ultrason.* SU-27 (6) (November 1980) 369.
- [19] J.-H. Jou, M.-Y. Han, D.-J. Cheng, *J. Appl. Phys.* 71 (9) (1 May 1992) 4333.
- [20] J.A. Thornton, *Thin Solid Films* 171 (1989) 5.
- [21] V.P. Kutepova, D.A. Hall, *Ultrason. Symp.* (1998) 213.
- [22] Q. Zhenxing, Z. Xiaozhong, Z. Mingzhou, W. Xizhang, L. Yujin, *IEEE Trans. Sonics Ultrason.* SU-32 (5) (September 1985) 630.
- [23] R.J. Lad, P.D. Funkenbusch, C.R. Aita, *J. Vac. Sci. Technol.* 17 (4) (Jul./Aug. 1980) 808.